Purification of Methylene Blue via Photocatalytic Nanofibrous Membranes Containing TiO_2 Nanoparticles

Ali Sajjadi, MSc, Seyed Abdolkarim Hosseini Ravandi, PhD, Hossein Izadan, PhD, Nastaran Kadivar, BSc

Department of Textile Engineering, Isfahan University of Technology, Isfahan IRAN

Correspondence to:
Seyed Abdolkarim Hosseini Ravandi email: hoseinir@cc.iut.ac.ir

ABSTRACT

In this paper, titanium dioxide nanoparticles were synthesized on polyacrylonitrile nanofiber membranes via a sol-gel process. Filter structure consisted of a non-woven polyurethane-carbon substrate, polyacrylonitrile nanofiber and titanium dioxide nanoparticles. The concentration of methylene blue dye solution was measured via UV radiation. The filtration efficiency was calculated via Langmuir-Hinshelwood pseudo-first order equations. The results showed that the filtration efficiency of samples using titanium dioxide under UV rays was higher than those without titanium dioxide and UV rays in both immersing and cross-flow processes. Degradation efficiency of the cross-flow system was three times higher than that of immersing method. In the cross-flow process, the effect of three variables-pressure on the membrane, initial concentration of dye solution and pH of the dye solution was studied under UV rays. The highest efficiency obtained was 90.3% by using 1.5 bar pressure, 40 μM initial concentration and pH of 4.1.

Keywords: catalysts, degradation, fibers, membranes, textiles, methylene blue.

INTRODUCTION

Textile industry wastewaters are widespread. Some are polluted with biological agents and can be remediated by simple wastewater treatment, while in the case of others even more extreme treatment methods may not be adequate [1, 2]. More severe environmental legislation for factories, and an increase in industrial production and consequently wastewater volume on the other increases the need for more sophisticated wastewater treatment systems for certain industrial units [3]. New environmental laws require wastewater treatment via surface absorbance prior to subsequent treatment stages. Solar and visible light driven photocatalysis treatment methods for wastewater treatment developed to date have not been adequate in reducing contaminants to required levels [4, 5].

The use of advanced oxidation processing offers a potential solution to industrial wastewater treatment. This approach is based on producing activated species such as hydroxyl radical that will react with and purify a wide range of industrial pollution. One type of advanced oxidation processing methods uses titanium dioxide [5, 6]. High photocatalytic function, long durability, high oxidation rates by holes in the band structure, relatively low price, being non-toxic and anticorrosion against light and chemicals are some advantages of using titanium dioxide as a semi conductive metallic oxide [7-11].

Titanium dioxide is activated via light energy which is higher than its energy gap equivalent of 32 electron volts. Therefore, titanium dioxide can be activated by ultraviolet rays or the UV spectrum of direct sunlight [3, 4, 7, 12]. Under such conditions, conduction band electrons and valance band holes are developed. These developed electrons participate in a reduction reaction of oxygen in the air adsorbed on the surface of the titanium dioxide and converts them into superoxide anion radical ($O_2^{\cdot-}$). Holes present in the valance band degrade existing water molecules in atmospheric moisture to hydroxyl radicals ($OH^{\cdot}$). The hydroxyl radicals participate in oxidation reactions with pollutant molecules that have organic functional groups and degrades them into less harmful materials to the environment e.g. water and carbon dioxide [3].

The maximum wavelength (λ) required for activating pure titanium dioxide is calculated as in Eq. (1) [13].

$$E_{(bg)} = \frac{hc}{\lambda} \quad (1)$$

Where $E_{(bg)}$, h and c are band gap energy, Planck constant and the speed of light, respectively. Therefore, the radiation wavelength required for surface activation of titanium dioxide will be less than or equal to 388 nm.

All photocatalytic reactions are demonstrated in the following steps and are similar for various organic contaminants [14].

1) $TiO_2 + h\nu(UV) \rightarrow TiO_2(e^-(CB) + h^+(VB))$

2) $TiO_2(h^+(VB)) + H_2O \rightarrow TiO_2 + H^+ + OH^-$

3) $TiO_2(h^+(VB)) + OH^- \rightarrow TiO_2 + OH^{\cdot}$ oxidation

4) $TiO_2(e^-(CB)) + O_2 \rightarrow TiO_2 + O_2^{\cdot -}$ reduction

5) $H^+ + O_2^{\cdot -} \rightarrow H_2O$

6) *Wastewater* + $OH^{\cdot}$ → *Degradation Product* $(CO_2, H_2O, \ldots)$

In the above equations, VB represents valance band and CB represents conduction band. The resulting hydroxyl radical has high oxidation properties and are capable of degrading organic molecules into less harmful materials [14].

Organic molecules, containing hydrogen and free negative anions in their structure possess a reducing property that enables them to participate in oxidation reactions with hydroxyl radicals, converting into more simple matter such as water and carbon dioxide [3]. Degradation of an organic molecule occurs at the weakest chemical bond among its functional groups.

The ultimate reaction of an organic molecule via a photocatalytic process is demonstrated by the following:

$$C_mH_nO_yX_z + (m + \frac{sz}{2} - \frac{kz}{4} - \frac{y}{2})O_2 \xrightarrow{UV+TiO_2} mCO_2 + (n - \frac{kz}{2})H_2O + zXO_s^{-k}$$

Where m, n, y, z, represent the number of atoms concerning C, H, O, X in the organic compound $C_mH_nO_yX_z$, respectively. *k* and *s* also represent the corresponding oxygen valence and stoichiometric ratio of oxygen in molecule XO_s, respectively. In the aforementioned chemical formula X can be a halide, nitrogen, phosphorus or sulfur [3].

Many investigations have been made into dye removal from wastewater via photocatalytic degradation processes. Kuo *et al.* [15] reported that the degradation of methylene blue dye could be achieved by attaching titanium dioxide powder particles 30 nm in size with lateral surface areas of 50±15 m^2/g to the impeller blades surface and inner surface of a reactor via resin. The experiment was done at pH= 4, 7, 10. It was observed that the dye removal rate was highest at pH of 4 due to an increase of $C_{16}H_{18}N_3S^-$ free anions in solution and a resulting increase in reduction rate [15]. Experiments were also performed at three dye concentrations. It was observed that an increase in dye concentration leads to a decrease in dye removal. It is claimed that this decrease is due to the coverage of the TiO_2 activated sites (valance band holes) by dye anions, which is resulted in a decrease in the amount of the hydroxyl radical production [15]. Experiments using ultraviolet lamps as well as direct sunlight were also performed and the effect of light intensity on dye removal was studied. An increase in sunlight intensity increased the efficiency of dye removal. This observation was reported to be related to the increase in the solution temperature and consequently to an increase in the reaction efficiency [15].

Ollis et.al. demonstrated the effect of light intensity on dye photocatalytic processes according to first-order equation and found that at light intensity between 0 and 20 mW, dye degradation rate has a linear relationship with light intensity. As radiated light intensity increases to 25 mW, dye degradation rate has direct relationship with I^2 while at light intensities of $I \geq 25$ mW, dye degradation rate has no relation to I [16].

The effect the lateral surface areas of nanoparticles of titanium dioxide fibers were studied by Jochen. By increasing the porosity of titanium dioxide nanofibers and decreasing fiber diameter, the outer surface area increases, resulting in an increase in contact of the photoactive regions (holes) with dye molecules and an increase in dye removal [17].

There are different methods for the removal of dye molecules from wastewater, including ozonation, biological treatment, adsorption, ion exchange, coagulation and membrane processes. Among these methods, the membrane process is more effective than the other methods. A membrane acts as a barrier separating two discrete phases. Its main function is to separate species which come into contact within one phase (feed) and transport them across to the other (permeate). Nanofibrous membranes produced by electrospinning offer unique properties such as high specific surface area, good interconnectivity of pores, high fluxes, and a potential to incorporate active chemistry or functionality at the nanoscale [18-21].

The aim of this research was to investigate the effect of TiO_2 nanoparticles on the efficiency of the photocatalytic degradation of methylene blue dye. A comparison of the dye removal efficiency was made between immersion and cross-flow filtration. Finally, the effect of initial dye concentration, membrane pressure and solution pH on the photo catalytic degradation efficiency of the methylene blue dye was investigated.

EXPERIMENTAL

The filter used in this study consists of three parts. Part one is a substrate made of polyurethane-carbon non-woven fabric produced by Iran's Milad Industry Company. Part two is a polyacrylonitrile nanofiber web produced via electrospinning on top of the substrate, and part three is a polyethylene net-like overlaying protective layer to prevent of nanofiber web condensation under pressure.

Polyacrylonitrile nanofibers were produced from a solution of 15 wt% PAN polymer (M_w=10^5 g/mol) made by Iran's PolyAcryl Company and DMF solvent made by Germany's Merck Company. Nanofibers were electrospun at 10 kV v, 0.26 ml/hr. feed rate, 15 cm spinning distance, 41% relative humidity, 20 °C temperature and 10 hour time length.

Synthesis of Titanium Dioxide Nanoparticles

In order to deposit titanium dioxide nanoparticles upon the nanofibers in the filter structure, a low temperature sol-gel process was used. In this case, two solutions were prepared. For the first solution, 12 ml titanium isopropoxide made by Germany's Merck Company was added to 50 ml 2-isopropanol solvent made by Germany's Merck Company and was stirred. Then 0.7 ml triethylamine made by Germany's Merck Company was added to this solution as a stabilizer. The solution was then put into a vacuum flask under neutral conditions in the presence of argon gas with a pressure of 1 bar. The solution was stirred for 15 minutes via electric mixer with a rate of 200 rpm.

Another solution was made by mixing 1 ml hydrochloric acid made by Germany's Merck Company, 0.5 ml water and 50 ml 2-isopropanol. The solution was stirred via electric mixer for 10 minutes. Next, both solutions were mixed and the final solution was stirred via electric mixer at a rate of 200 rpm, under neutral conditions in the presence of 1 bar argon gas for 60 minutes to prepare the gel [22].

The gel was then poured into a broad dish and electrospun nanofibers were wet impregnated in the for 5 minutes. After extracting the nanofibers from the gel, they were put into a 70 °C oven for 1 hour to evaporate the solvent. In order to complete the titanium dioxide structure formation, nanofibers were put into a 120 °C oven for 30 minutes. Finally, the nanofibers were rinsed with distilled water to separate non-sticking nanoparticles from the nanofiber's surface [22].

Methylene blue dye ($C_{16}H_{18}N_3SCl$) in the form of powder made by China's Yuhao Company was dissolved in distilled water at a concentration of 40 µM. This dye was chosen because it reacts rapidly in the presence of oxygen [23]. The dye structure is shown in *Figure 1*.

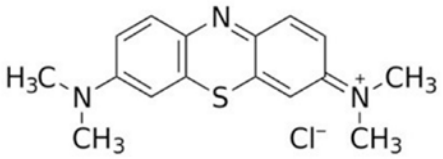

FIGURE 1. Methylene blue dye structure (C.I. 52015)

In order to perform photocatalytic reactions to degrade the methylene blue dye, a UV lamp made by Netherland's Philips Company with 254 nm wavelength and 0.085 W radiant power was used.

Measuring Dye Solution Concentration

For the concentration measurement of the methylene blue dye solution, a Shimadzu transmission spectrophotometer device, model UV mini -1240, was used. This device is based on Beer-Lambert law from Eq. (2) [24].

$$A = -\log(\frac{I}{I_0}) = \varepsilon LC \quad (2)$$

In this equation, A represents absorption amount, I_0 is radiated light intensity, I is the intensity of light transmitted from solution, $\mathcal{E}$ represents the molar extinction coefficient, L is cell length and C is solution concentration. A dye solution with a specific concentration was prepared, its absorption was measured in the visible region from wavelength of 400 to 780 nm via a transmission spectrophotometer and the maximum absorption wavelength for the dye solution was calculated.

According to Eq. (2), dye solution absorbance based on the Beer-Lambert law is directly related concentration. Dye solutions with concentrations of 25, 30, 35, 40, 45, 50, 55, 60 µM were prepared and their absorbency at the maximum wavelength of dye's absorbance, 668.5 nm, was measured.. Concentration and absorbency coordinates were input to SPSS software to obtain Beer-Lambert law correlations via linear regression. Using the obtained linear equation, dye concentrations can be calculated. In order to determine the extent of the of the dye oxidation reaction, a first-order equation of chemical equilibrium based on Longmuir-Hinshelwood theory was used, as shown by Eq. (3).

$$\ln \frac{c_0}{c} = kt \tag{3}$$

In Eq. (3) c_0 represents dye solution primary concentration in molar unit, c expresses dye solution concentration at time length t, k represents the first-order reaction progress constant in terms of min^{-1} and t states time in terms of min [14].

Eq. (4) was used to determine filtration dye removal efficiency at the time length equal of t.

$$\%Eff = \frac{c_0 - c_t}{c_0} \times 100 \tag{4}$$

In Eq. (4), c_0 represents initial concentration of the dye in the wastewater and c_t represents the dye concentration in the wastewater in time length t after filtration process inception [14].

Filtration Via Immersion Method

Experiments were divided into two categories. The first type involved an immersion process. In order to perform the immersion process, 100 cc methylene blue dye solution with a concentration of 40 µM was poured into three different beakers. Beaker number one contained 4×4 cm^2 cuttings of polyacrylonitrile fibers plus the substrate. Beakers two and three held 4×4 cm^2 cuttings of polyacrylonitrile fibers with titanium dioxide nanoparticles plus the substrate. Beaker No. 3 was exposed to UV radiation during the experiment. *Table I* shows experimental sample specifications.

TABLE I. Experimental sample specifications for the immersion process.

Sample Number	Filter Structure
1	electrospun PAN on urethane-carbon substrate
2	electrospun PAN with TiO_2 nanoparticles on urethane-carbon substrate
3	electrospun PAN with TiO_2 nanoparticles on urethane-carbon substrate and UV irradiation

To measure dye removal efficiency a 1 cc sample of methylene blue dye solution was removed from each beaker every 20 minutes for 3 hours. After the absorbency was measured, the measured sample was returned to the beaker to maintain a constant solution volume remained throughout the experiment. Next, the solution concentrations versus time were calculated via the Beer-Lambert law and the filtration efficiency was determined. Finally reaction progress constants were determined using first-order equilibrium equations. The experiment was repeated three times and the averages of the results were reported.

For all experiments done for the immersion process, pH of the dye solutions remained constant at 6.4, dye solution retention time before filtration was 24 hours and the initial concentration of dye solutions was 40 µM.

Filtration Via Cross-Flow Method

The second type of experiments were carried out using a cross flow process, as shown in *Figure 2*. In this process the feed flow moves parallel to the membrane surface and splits into two flows i.e. filtered flow and remaining flow.

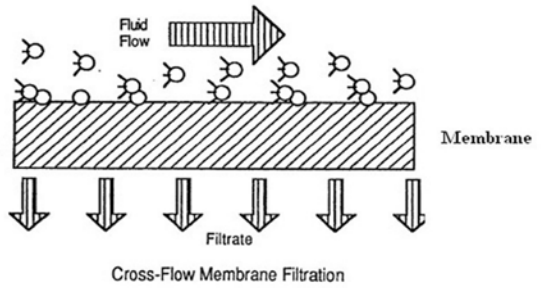

FIGURE 2. Schematic view of cross flow filtration mechanism.

The specific layout of components used in this study is displayed in *Figure 3*. Filtration was carried out in a single-stage process using re-circulation. Re-circulation flow was maintained at a constant pressure by means of an adjustable pump. Samples as shown in were exposed to UV radiation provided by a source while inside a clear cubic glass container with dimensions of 12×8 cm^2.

Dye solution samples were collected every 5 minutes for 1 hour, absorption was measured, concentrations as a function of time were determined from the Beer-Lambert law were calculated and filtration efficiencies were calculated. Finally reaction progress constants were determined using first-order equilibrium equations. The experiment was repeated three times and the averages of the results were reported.

For all immersion process experiments, pH of the dye solutions remained constant at 6.4, dye solution retention time before filtration was 24 hours and the initial concentration of dye solutions was 40 µM and 1.5 bars pressure was maintained on the membrane. The effects of initial dye solution concentration, pressure on the membrane and the pH of the dye solution on the photocatalytic degradation efficiency were studied.

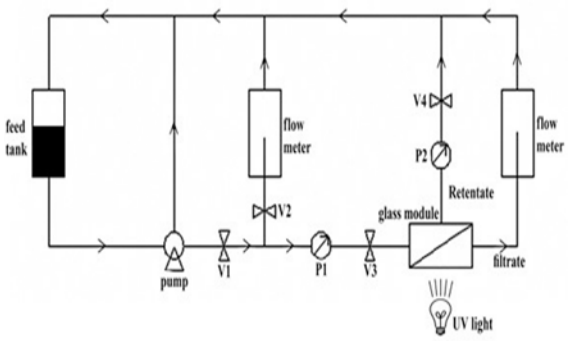

FIGURE 3. Components placement layout in cross flow filtration system v_1, v_2, v_3, v_4 represent valves used, P_1, P_2 represent pressure indicators used and flow meters represent existing routes for flow measurements in system.

To study the initial dye concentration effect on filtration efficiency, three concentrations of methylene blue dye (40, 50 and 60 µM) were prepared. The filter containing titanium dioxide nanoparticles and PAN nanofiber was placed under UV irradiation in the glass container throughout the filtration process. To study the effect of pressure on the membrane on the filtration efficiency, the filter containing titanium dioxide nanoparticles and PAN nanofiber was placed under continuous radiation of UV in membrane container at pressures of 1.3, 1.5 and 1.7 bars. Eq. (5) was used to calculate the pressure on membrane.

$$\Delta p = \frac{p_1 + p_2}{2} + p_{atm} \quad (5)$$

In this equation, P_1 and P_2 represent pressures read from indicators placed before and after membrane holder, respectively, and P_{atm} was considered 1 bar. To study the effect of the methylene blue dye solution pH on the filtration efficiency, the pH of the dye solutions was set to 6.4, 4.1 and 10.5. The pH of the dye as received is 6.4. Solutions of hydrochloric acid and soda at 0.1 M concentration were used to adjust the pH of the solution for this part of the study.

UV irradiation was continuously during experiments involving all three of the variables studied using the cross flow filtration process. Dye solution samples were collected every 5 minutes for 1 hour, absorption was measured, concentrations as a function of time were determined from the Beer-Lambert law were calculated and filtration efficiencies were calculated. Finally reaction progress constants were determined using first-order equilibrium equations. Digital images of nanofibrous membranes containing TiO_2 nanoparticles before and after methylene blue removal experiments are shown in *Figures 4 & 5.*

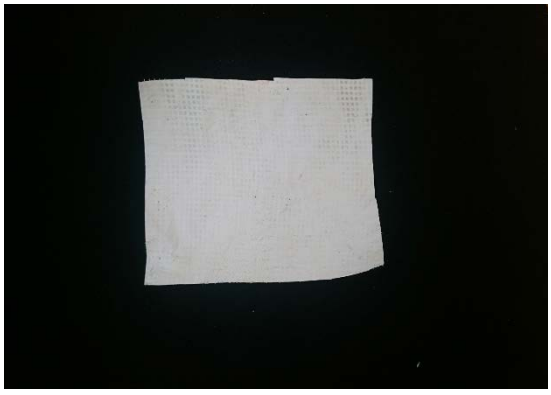

FIGURE 4. Nanofibrous membranes containing TiO_2 nanoparticles before methylene blue removal experiments.

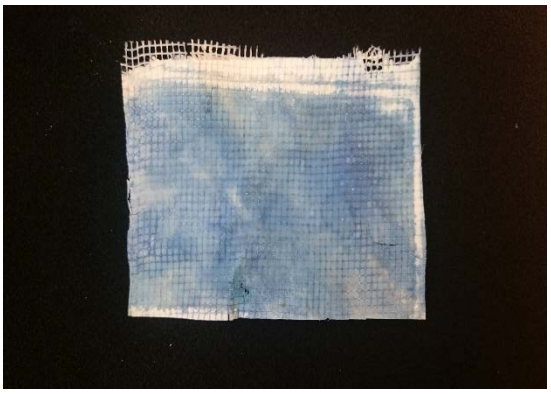

FIGURE 5. Nanofibrous membranes containing TiO_2 nanoparticles after methylene blue removal experiments.

Characterization

The structure of the filter layers was captured visually via field emission scanning electron microscopy (FESEM), using a HITACHI S.4160 instrument. Statistical analyses of 100 fiber diameters and 15 filter substrate pores were completed via Digimizer software. To study the crystal structure of titanium dioxide nanoparticles, X-ray scattering spectroscopy measurements were conducted using a Philips X'pert-MPD instrument. A copper target tube and a 1.54 angstrom X-ray wavelength were used. Results were analyzed via PANalytical X'pert Highscore software. In order to study the functional groups of the methylene blue dye before and after the filtration process, Fourier transform infrared (FTIR) spectroscopy was carried out using Bomem MB100 spectrophotometer. Results were analyzed via Win-Bomem Easy software.

RESULTS AND DISCUSSION

SEM Analysis

FESEM images of the nanofiber structure along with the diameter distribution curve are shown in *Figure 6*. Nanofiber average diameters are 531.8 nm with a CV of 13.87% according to the distribution curve in *Figure 7*.

An FESEM image of the titanium dioxide nanoparticles upon membrane structure is shown in *Figure 8*. Average diameter of these nanoparticles is estimated to be 53 nm with a CV of 24.33% according to microscopic images.

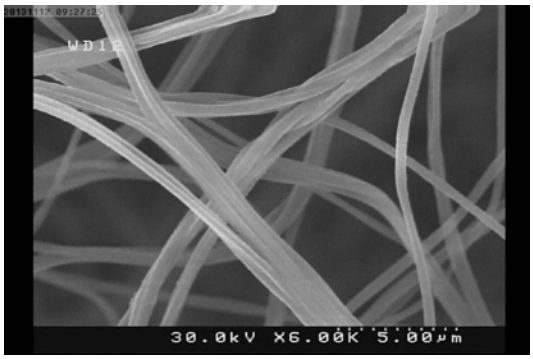

FIGURE 6. Filter nanofiber structure at 6000 times magnification.

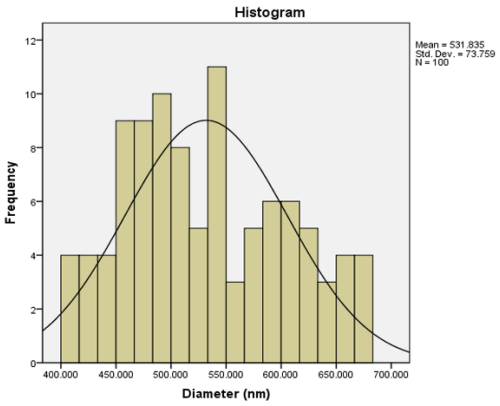

FIGURE 7. Nanofiber diameter distribution curve.

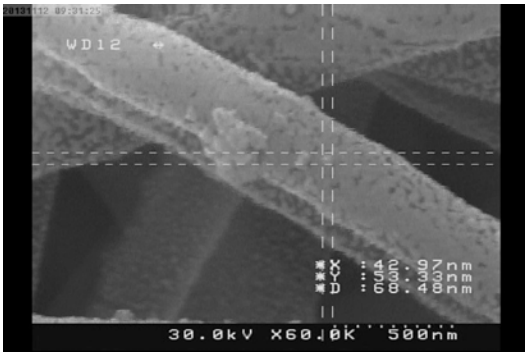

FIGURE 8. Titanium dioxide nanoparticles structure upon nanofibers of 60000 times magnification.

Thickness Determination

Thickness of the membrane was determined to be 200 µm. The carbon-polyurethane substrate used was 1.9 mm thick. Total thickness of filter was calculated to be about 2.1 mm.

X-Ray Diffraction (XRD) and FTIR Analysis

In *Figure 9*, the XRD spectrum of titanium dioxide nanoparticles is shown. Analyzing the results indicates that two peaks in the curve related to the anatase phase. This confirms the presence of photocatalytic properties in the membrane structure.

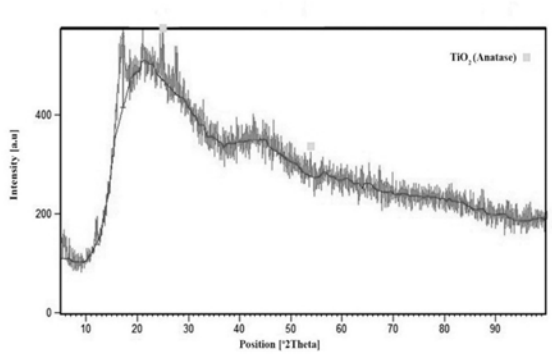

FIGURE 9. Membrane XRD spectra.

In *Figure 10*, the FTIR spectra of methylene blue dye before and after filtration is shown. Analyzing the results indicates that the six peaks existing in the curve before methylene blue dye filtration disappeared after photocatalytic filtration of methylene blue dye. In *Table II*, the names of identifiable degraded functional groups are mentioned according to methylene blue dye introduced structure from *Figure 1*, along with associated frequencies.

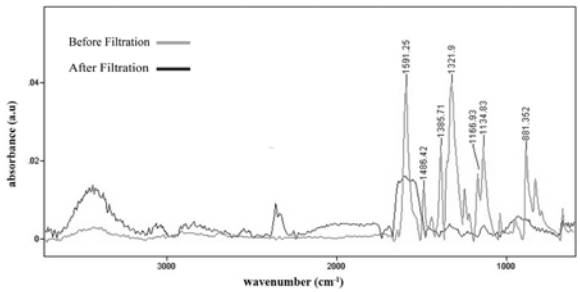

FIGURE 10. Methylene blue dye FTIR spectra before and after photocatalytic filtration.

TABLE II. Methylene blue dye degraded functional groups after filtration.

Functional Group	Wave number (cm^{-1})
C-S	1166.93 and 1134.83
C-N	1321.9
CH_3	1486.42 and 1385.71
C=C	1591.25

Dye Calibration Curve

Methylene blue dye solution absorbency at a concentration of 40 µM and pH of 6.4 without addition of acid or base was measured. Maximum wavelength of absorbency in this case was noted 668.5 nm. At pH of 4.1 the maximum wavelength of absorbency was 651 nm and at pH of 10.5 the maximum wavelength of absorbency was 638.5 nm.

Dye calibration curves calculated from Eq. (2) for each pH solution as a function of concentration are shown in *Figure 11*. Linear regression methods were used to obtain a best fit line equation for the experimental points [25].

Concentration of dye in the wastewater samples at each pH was obtained via Eq. (6), (7) and (8). According to the literature, theoretically there should be no intercept for the equations. However violation of Beer-Lambert as a result of dye aggregation, stray light and quantization errors will cause an intercept [25].

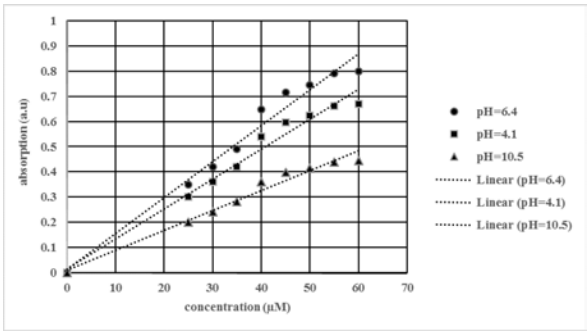

FIGURE 11. Dye calibration curve.

$$A = 0.014C + 0.010 \quad \text{pH=6.4} \quad (6)$$

$$A = 0.012C + 0.014 \quad \text{pH=4.1} \quad (7)$$

$$A = 0.008C + 0.010 \quad \text{pH=10.5} \quad (8)$$

Immersion Process

Filtration efficiencies from Eq. (4) for the immersion process are shown in *Figure 12*. According to *Figure 12*, sample 3, which undergoes significant dye degradation under the photocatalytic processes, shows the highest filtration efficiency over the 3 hours of run time. In the two other samples, dye saturation occurs and the filtration efficiency almost stayed constant or increased negligibly. Therefore, an increase in the filtration efficiency due to the photocatalytic process is confirmed.

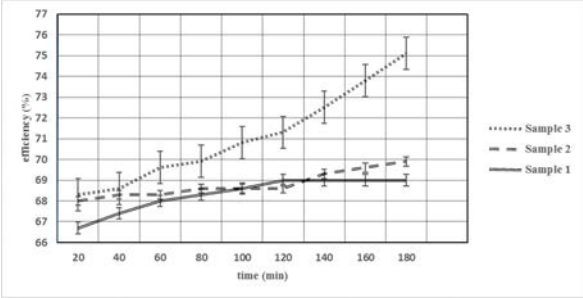

FIGURE 12. Filtration efficiency of three different samples in immersing process

An ANOVA test was carried out on the filtration efficiency data using SPSS software. The results confirmed a statistically significant difference between sample 3 and the other two samples.

In order to study the photocatalytic reaction progress rate for sample 3 according to Eq. (3), the natural logarithm of C_0/C, ln (C_0/C) values are plotted in *Figure 13*. The equilibrium constant equation was obtained by linear regression and is shown in Eq. (9).

$$\ln \frac{c_0}{c} = 0.001t + 1.099 \qquad (9)$$

From Eq. (9) the index for the reaction rate, k, is equal to 0.001 min^{-1}.

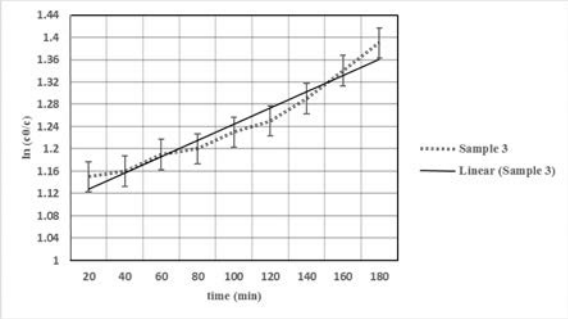

FIGURE 13. Ln (C_0/C) values for sample 3 in terms of time.

Cross-Flow Process

The results of the filtration efficiency via Eq. (4) for the cross-flow process are given in *Figure 14*. According to *Figure 14* sample 3, which undergoes significant dye degradation under the photocatalytic processes, shows the highest filtration efficiency over the 3 hours of run time. In the two other samples, dye saturation occurs and the filtration efficiency almost stayed constant or increased negligibly. Therefore, an increase in the filtration efficiency due to the photocatalytic process is confirmed.

An ANOVA test was carried out on the filtration efficiency data using SPSS software. The results confirmed a statistically significant difference between sample 3 and the other two samples. Also, an LSD test showed that there is a significant difference between the filtration efficiency average of sample 3 and the other samples..

By comparing *Figure 12* and *Figure 14* it can be concluded that the cross-flow process reached an efficiency of 77.7% in 60 minutes while the immersion process reached an efficiency equal of 75.1% in 180 minutes. The reason for this difference is the pressure on membrane in the cross-flow process, which causes an increase in the filtration efficiency.

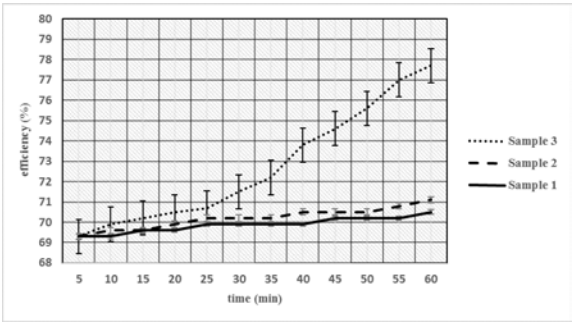

FIGURE 14. Filtration efficiency of three different samples in cross-flow process.

In order to study the photocatalytic reaction progress rate for sample 3 according to Eq. (3), ln (C_0/C) values are given in *Figure 15*. The equilibrium constant equation is computed by a linear regression method and is shown in Eq. (10).

$$\ln \frac{c_0}{c} = 0.006t + 1.113 \qquad (10)$$

From Eq. (9) the index for the reaction rate, k, is equal to 0.006 min^{-1}. Comparison of the calculated k values for the cross-flow process (0.006) immersion process (0.001), indicates that the photocatalytic reaction progress rate in the cross-flow process is nearly 6 times greater than in the immersion process.

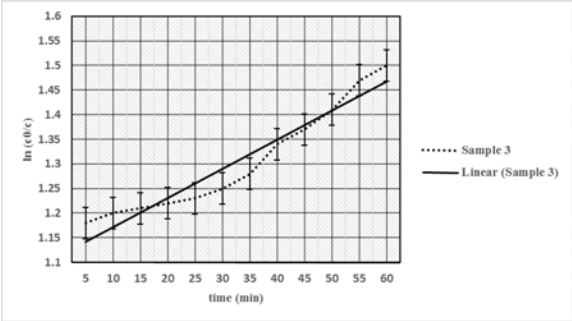

FIGURE 15. Ln (C_0/C) values in terms of time for sample 3.

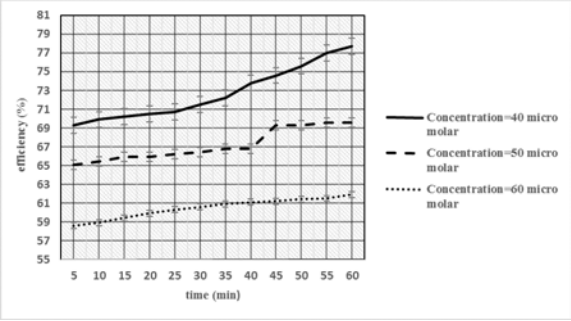

FIGURE 16. Filtration efficiency of three different samples from the concentration experiment in the cross-flow process.

By extrapolating the data shown in *Figure 13* and *Figure 15* using the efficiency equations and the equation for the first-order equilibrium of each process, it is observed that in the immersion process, filtration efficiency of 85% is obtained after 798 minutes, while the same rate of efficiency in cross-flow process is obtained after about one sixth of the time i.e. 132 minutes. Therefore, the cross-flow process would be preferred over immersion process.

Existence on intercepts in the data generated using Eq. (9) and Eq. (10) shows that the dye degradation occurs through two different mechanisms. Initially, dye removal occurs via the carbon-polyurethane substrate and polyacrylonitrile nanofibers. In the second stage, dye removal occurs through the photocatalytic process and oxidation reactions according to Langmuir-Hinshelwood model [26].

Experiments to determine the effects of dye solution initial concentration, pressure on membrane and dye solution pH on photocatalytic filtration efficiency were carried out on Sample 3 in the cross-flow process. Repeat experiments are designated by an asterisk (*) sign.

Dye Solution Initial Concentration Effect

The filtration efficiencies at concentrations of 40 µM (sample 4), 50 µM (sample 5) and 60 µM (sample 6) via Eq. (3) are plotted in *Figure 16*. As concentration increases, the dye removal efficiency decreases. This is a result of an increase in percentage of ions percentage in dye molecules. This tends to limit photoactive species such as hydroxyl radicals [14, 27].

The ANOVA statistical test showed that there is a significant difference between filtration efficiency values of samples 5 and 6. The LSD test showed that no significant difference exists due as a result of interactions between metal radicals and dye ions.

To determine the photocatalytic reaction progress rates, ln (C_0/C) values for samples 4 to 6 were calculated and shown in *Figure 17*. First-order equilibrium equations for the three samples were obtained as Eq. (11), (12) and (13).

$$\ln\frac{c_0}{c} = 0.006t + 1.113 \quad \text{*Related to sample 4} \quad (11)$$

$$\ln\frac{c_0}{c} = 0.003t + 1.025 \quad \text{Related to sample 5} \quad (12)$$

$$\ln\frac{c_0}{c} = 0.001t + 0.880 \quad \text{Related to sample 6} \quad (13)$$

According to the Eq. (11), (12) and (13), the photocatalytic reaction rate in sample 4 is about 2 times that of sample 5 and about 6 times that of sample 6. This is due to a decrease in hydroxyl radical activity as a result of interactions of the dye ions as dye concentration increases [14, 27].

Intercepts are obtained for Eq. (11), (12) and (13) due to the first-stage of the two-stage absorbance mechanism explained in the previous section. The ANOVA showed that there is not a significant difference between intercept values at a 95%

confidence level. The intercept values have random fluctuations at the initial concentration values. This is likely due to a small amount of polyacrylonitrile nanofiber in the filter structure, low absorption capability of polyacrylonitrile nanofiber at ambient temperature and repeatability errors of the spectrophotometer and cross flow apparatus.

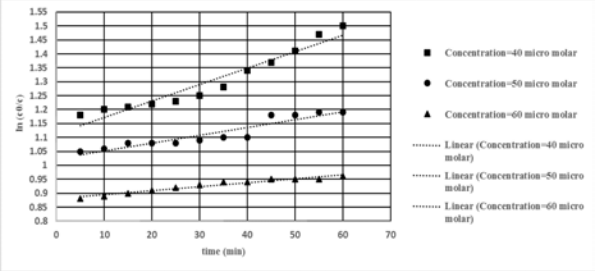

FIGURE 17. Ln (C_0/C) values in terms of time in three different concentrations.

Pressure On Membrane Effect

The filtration efficiencies calculated from Eq. (4), for pressures of 1.3 bar (sample 7), 1.5 bar (sample 8) and 1.7 bar (sample 9) are given in *Figure 18*. An increase in the pressure from 1.3 bar to 1.5 bar and from 1.5 bar to 1.7 bar results in higher filtration efficiency due to the compression of pores in the membrane as well as membrane compaction.

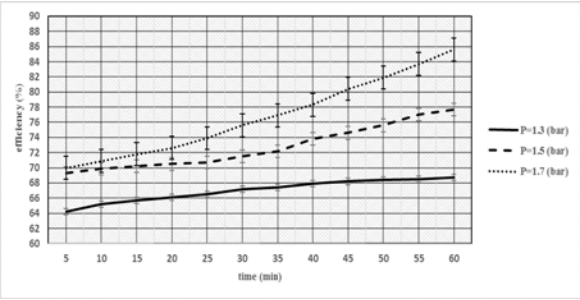

FIGURE 18. Filtration efficiency in the three different pressures in the cross-flow process.

ANOVA statistical analysis and the LSD test showed that there is a significant difference between the filtration efficiency values.

To determine the photocatalytic reaction progress rates, ln (C_0/C) values for samples 7 to 9 were calculated, and the results are shown in *Figure 19*.

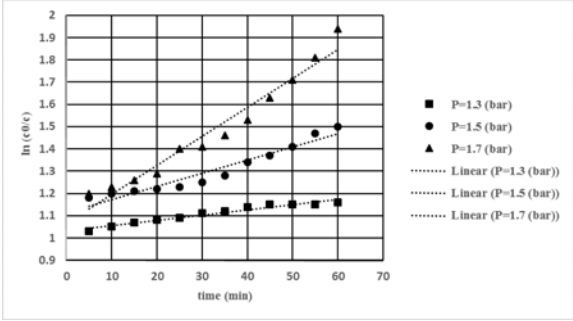

FIGURE 19. Ln (C_0/C) values in terms of time in the three different pressures.

The first-order equilibrium equations for the three samples were obtained and are shown, respectively, in Eq. (14), (15) and (16).

$$\ln\frac{c_0}{c} = 0.002t + 1.031 \qquad \text{Related to sample 7} \quad (14)$$

$$\ln\frac{c_0}{c} = 0.006t + 1.113 \qquad \text{Related to sample 8*} \quad (15)$$

$$\ln\frac{c_0}{c} = 0.013t + 1.065 \qquad \text{Related to sample 9} \quad (16)$$

From the equations, as pressure increases from photocatalytic reaction rate at 1.5 bar is about 3 times the rate at 1.3 bar, and the rate at 1.7 bar is about twice the rate at 1.5 bar. The reason for the decrease in rate change is decreasing membrane compressibility with increasing pressure.

Intercepts are obtained for Eq. (14), (15) and (16) due to the first-stage of the two-stage absorbance mechanism explained in the previous section. The ANOVA results showed that there is no significant difference between intercept values at 95% confidence level.

Dye Solution pH Effect

The filtration efficiencies calculated from Eq. (4) at pH values of 4.1 (sample 10), 6.4 (sample 11) and 10.5 (sample 12) are given in *Figure 20*. The photocatalytic filtration efficiency decreases as solution pH increases. It is assumed that as pH increases, the concentration of OH^- ions also

increases. Consequently the oxidation reaction rate, which leads to hydroxyl radical production, will increase and therefore dye degradation will occur at a higher rate. However, it is notable that a pH increase above a certain level will cause an increase in columbic repulsive forces between the photocatalyst charged surface with negative potential and OH^- ions. This results in an increase in the dye absorbance rate on the filter and a decrease in hydroxyl radical generation. In other words, at pH of 10.5 the dominant mechanism in dye degradation is columbic repulsive forces, resulting in an increase in OH^- concentration in the solution [28-33].

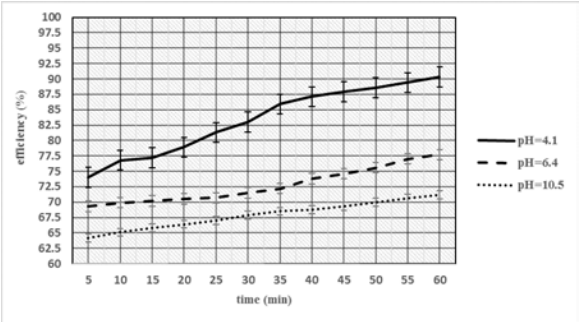

FIGURE 20. Filtration efficiency in the three different pH values in the cross-flow process.

A more reasonable mechanism for explaining this aforementioned phenomenon is that at high pH values an increase in OH^- concentration causes a reaction between individual hydroxyl radicals, leading to the development of ion-radical pairs. This reaction causes the OH^- ions to cover surrounding hydroxyl radicals and the dye degradation reaction to be decreased with a resulting decrease in the filtration efficiency. At an acidic pH of 4.1, the dominant absorbance mechanism is columbic attractive forces between the photocatalyst surface and the dye solution with positive potential and OH^- form [28-33].

Thus, the dominant mechanism of dye degradation and maximum dye degradation differ in acidic and basic solutions with sample 10, the most acidic solution showing the highest rate. that The ANOVA and LSD tests showed that there is a significant difference between the filtration efficiency values.

To determine the photocatalytic reaction progress rate, ($\ln C_0/C$) value for samples 10 to 12 was calculated. Results are given in *Figure 21*. The first-order equilibrium equations were computed and are shown in Eq. (17), (18) and (19).

$$\ln \frac{c_0}{c} = 0.019t + 1.240 \quad \text{Related to sample 10} \quad (17)$$

$$\ln \frac{c_0}{c} = 0.006t + 1.113 \quad \text{Related to sample 11*} \quad (18)$$

$$\ln \frac{c_0}{c} = 0.004t + 1.015 \quad \text{Related to sample 12} \quad (19)$$

It is noteworthy that due to the same experimental conditions, Eq. (10), Eq. (11), Eq. (15) and Eq. (18) are the same.

From Eq. (17)-(19), the photocatalytic reaction rate of the sample 10 is more than three times of that of the sample 11 and almost 5 times more than that of the sample 12. This is a result of the hydroxyl radicals being covered by OH^- ions at high pH values. This causes a decrease in reactions between hydroxyl radicals and dye molecule. In the case of acidic pH, the attraction between OH^- and positively charged dye molecules increases, leading to to an increase in the dye degradation rate.

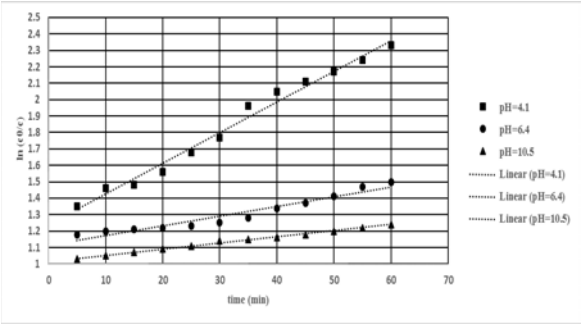

FIGURE 21. Ln (C_0/C) values in terms of time in the three different pH values.

Intercepts are obtained for Eq. (17), (18) and (19) due to the first-stage of the two-stage absorbance mechanism explained in the previous section. The ANOVA results showed that there is not a significant difference between intercept values at a 95% confidence level.

CONCLUSION

In this study, the effect of TiO_2 nanoparticles on the efficiency of the photocatalytic degradation of methylene blue dye using Langmuir-Hinshelwood model was investigated. The results showed that in the two methods of filtration; immersing and cross-flow processes, the filtration efficiency of samples

using titanium dioxide under UV rays was higher than that of the samples without titanium dioxide and without the presence of UV rays. Also with the same assumptions, degradation efficiency of the cross-flow system was more than 3 times higher than the immersing one. In the cross-flow test, the effect of three variables; pressure on the membrane, initial concentration of the dye solution and pH of the dye solution was studied. ANOVA and LSD tests showed that there are significant differences between efficiency values. The highest efficiency obtained was 90.3% at 1.5 bar pressure, 40 μM initial concentration, and pH of 4.1. Solution pH had the highest effect among the three variables on removal efficiency. As pH decreased from from 10.5 to 4.1, the photocatalytic reaction rate increases about 5 times.

REFERENCES

[1] Bajpai, S. K.; Thomas, V; Bajpai, M. "Novel Strategy for Synthesis of ZnO Microparticles Loaded Cotton Fabrics and Investigation of their Antibacterial Properties", *Journal of Engineered Fibers and Fabrics*, 6, Issue 3, 2011, pp.73-81.

[2] El Ghali, A; Hassen, B. M.; Sadok, R. M. "Surface Functionalization of Cellulose Fibers Extracted From Juncus Acutus L Plant: Application for the Adsorption of Anionic Dyes from Wastewaters", *Journal of Engineered Fibers and Fabrics*, 10, Issue 1, 2015, pp.52–62.

[3] Jinkai, Z. "Modified Titanium Dioxide (TiO_2) photocatalysts for the degradation of organic pollutants in wastewater", PHD thesis, Department of Chemical and Biomolecular Engineering, National University of Singapore, 2007.

[4] Chowdhury, P. "Solar and visible light driven photocatalysis for sacrificial hydrogen generation and water detoxification with chemically modified TiO_2", Department of Chemical and Biochemical Engineering. Thesis, The University of Western Ontario London, Ontario, Canada, 2012.

[5] Kondarides, D.I. "Photocatalysis", *Encyclopedia of Life Support Systems (EOLSS)*, University of Patras, Greece, 2010.

[6] Barros, A., Domingos, A., Fechine, P., Keukeleire, D. and Nascimento, R. "PET as a support material for TiO_2 in advanced oxidation processes", *Journal of applied polymer science*, 131, Issue 9., 2014.

[7] Schiavello, M. "Heterogeneous photocatalysis", *Wiley: NewYork*, 1997.

[8] Fujishima, A. N.; Rao, T.A.; Tryc, T. "Titanium Dioxide photocatalysis", *Journal of photochemistry and photobiology*, 1, No 1., 2000, pp.1-21.

[9] Shirsath, D.S.; Shrivastava, V.S. "Photocatalytic removal of O-Nitro Phenol from wastewater by novel an eco-friendly magnetic nanoadsorbent", *Int. J. Environ. Res*, 9, No 1., 2015, pp.363–372.

[10] Fallah Moafi, H.; Fallah Shojaie, A.; Zanjanchi, M.A. "Photoactive behavior of polyacrylonitrile fibers based on silver and zirconium co-doped titania nanocomposites: Synthesis, characterization, and comparative study of solid-phase photocatalytic self-cleaning", *Journal of applied polymer science*, 127, Issue 5., 2012, pp.3778-3789.

[11] Subha, P.P.; Jayaraj, M.K. "Solar photocatalytic degradation of methylorange dye using TiO_2 nanoparticles synthesised by sol–gel method in neutral medium", *Journal of Experimental Nanoscience*, 10, No. 14., 2015, pp.1106–1115.

[12] Fujishima, A. "Discovery and applications of photocatalysis creating a comfortable future by making use of light energy", *Japan nanonet bulletin*, Issue 44., 2005.

[13] Georgieva, J.; Valova, E.; Armyanov, S.; Philippidis, N.; Poulios, I.; Sotiropoulos, S. "Bi–component semiconductor oxide photoanodes for the photoelectrocatalytic oxidation of organic solutes and vapours: A short review with emphasis to TiO_2–WO_3 photoanodes", *Journal of Hazardous Materials*, 211, 2012, pp.30–46.

[14] Rashed, M.N.; El.Amin, A.A. "Photocatalytic degradation of methyl orange in aqueous TiO_2 under different solar irradiation sources", *International Journal of Physical Sciences*, 2, No. 3., 2007, pp.073–081.

[15] Kuo, W.S.; Ho, P.H. "Solar photocatalytic decolorization of methylene blue in water", *Journal of Chemosphere*, 45, 2001, pp.77–83.

[16] Ollis, D.F.; Pelizzetti, E.; Serpone, N. "Destruction of water contaminants", *Environ. Sci. Technol*, 25, 1991, pp.1523-1529.

[17] Jochen, W. "Titanium Dioxide", *Hannover Vincentz networ*k, 2003, pp.30–31.

[18] Chegoonian, P.; Feiz, M.; Hosseini Ravandi, S.A.; Mallakpour, S. “Preparation of Sulfonated Poly(ethylene terephthalate) Submicron Fibrous Membranes for Removal of Basic Dyes”, *Journal of Applied Polymer Science*, 124, 2012, pp.190–198.

[19] Ramakrishna, S.; Fujihara, K.; Teo, W.E.; Lim, T.C.; Ma, Z. “An Introduction to Electrospinning and Nanofibers”, *World Scientific: Singapore*, 2005.

[20] Garg, V.K.; Amita, M.; Kumar, R.; Gupta, R. “Basic dye (methylene blue) removal from simulated wastewater by adsorption using Indian Rosewood sawdust: a timber industry waste”, *Dyes and Pigments*, 63, No 3., 2004, pp.243–250.

[21] Gopal, R.; Kaur, S.; Ma, Z.; Chan, C.; Ramakrishna, S.; Matsuura, T. “Electrospun nanofibrous filtration membrane”, *Journal of Membrane Science*, 281, Issues 1-2., 2006, pp.581-586.

[22] Fallah Moafi, H.; Fallah Shojaie, A.; Zanjanchi, M.A. “Photoactive polyacrylonitrile fibers coated by nano-sized titanium dioxide: synthesis, characterization, thermal investigation”, *J. Chil. Chem. Soc*, 56, 2011, pp.610–615.

[23] Tabbara, M.A.; El Jamal, M.M. “A kinetic study of the discoloration of methylene blue by Na_2SO_3, comparision with NaOH”, *Journal of the University of Chemical Technology and metallurgy*, 47, No 3., 2012, pp.275–282.

[24] Thatipamala, R.; Hill, G. A.; Rohani, S. “Absorption of Radiation by Substances at “High” Concentrations: A New Equation and Process Monitoring Applications”, *The Canadian Journal of Chemical Engineering*, 71, 1993, pp.977–981.

[25] Gunay, M.; Jasper, W.J. “Limitations in predicting dyebath exhaustion using optical spectroscopy”, *Coloration Technology*, 126, Issue 3, 2010, pp.140–146.

[26] Mohamed, E.F. “Removal of organic compounds from water by adsorption and photocatalytic oxidation”, University of Toulouse, 2011.

[27] Poulios, I.; Tsachpinis, I. “Photodegradation of the textile dye reactive black 5 in the presence of semiconducting oxides”, *J. Chem. Technol. Biotechnol.*, 74, 1999, pp.349–357.

[28] Akpan, U.G.; Hameed, B.H. “Parameters affecting the photocatalytic degradation of dyes using TiO_2-based photocatalysts: A review”, *Journal of Hazardous Material*, 170, 2009, pp.520–529.

[29] Tang, W.Z.; An, H. “UV/TiO_2 photocatalytic oxidation of commercial dyes in aqueous solutions”, *Chemosphere*, 31, 1995, pp.4158–4170.

[30] Tang, W.Z.; An, H. “Photocatalytic degradation kinetics and mechanism of acid blue 40 by TiO_2/UV in aqueous solution”, *Chemosphere*, 31, 1995, pp.4171–4183.

[31] Alaton, I.A.; Balcioglu, I.A. “Photochemical and heterogeneous photocatalytic degradation of waste vinylsulphone dyes: a case study with hydrolyzed Reactive Black 5”, *J. Photochem. Photobiol. A: Chem*., 141, 2001, pp.247–254.

[32] Poulios, I.; Aetopoulou, I. “Photocatalytic degradation of the textile dye Reactive Orange 16 in the presence of TiO_2 suspensions”, *Environ. Technol.*, 20, 1999, pp.479–487.

[33] Poulios, I.; Avrans, A.; Rekliti, E.; Zouboulis, A. “Photocatalytic oxidation of Auramine O in the presence of semiconducting oxides”, *J. Chem. Biotechnol.*, 75, 2000, pp.205–212.

AUTHORS’ ADDRESSES

Ali Sajjadi, MSc
Seyed Abdolkarim Hosseini Ravandi, PhD
Hossein Izadan, PhD
Nastaran Kadivar, BSc
Department of Textile Engineering
Isfahan University of Technology
Isfahan 84156-83111
IRAN